

## INNOVATIVE SOLUTIONS FOR LONG-SPAN SUSPENSION BRIDGES

**Gianni Bartoli<sup>\*</sup>, Piero D'Asdia<sup>†</sup>, Sofia Febo<sup>†</sup>,  
Claudio Mannini<sup>\*</sup>, Stefano Pastò<sup>\*</sup> and Lorenzo Procino<sup>\*</sup>**

<sup>\*</sup>CRIACIV/Dipartimento di Ingegneria Civile e Ambientale  
Università degli Studi di Firenze, Via S. Marta 3, 50139 Firenze, Italy  
e-mails: gbartoli@dicea.unifi.it, claudio.mannini@dicea.unifi.it,  
stefanop@dicea.unifi.it, lorenzo.procino@pin.unifi.it

<sup>†</sup>CRIACIV/Dipartimento di Progettazione, Riabilitazione e Controllo delle Strutture Architettoniche  
Università di Chieti-Pescara, Viale Pindaro 42, 65127 Pescara, Italy  
e-mails: pidasdia@tin.it, s.febo@unich.it

**Keywords:** Aeroelasticity, Bridges, Multiple-box girder, Innovative solutions, Wind-tunnel tests, Aerodynamic optimization

**Abstract:** *Due to the reduced separation between vertical and torsional natural modes, bridges with central spans beyond 1000-1500 m have to be designed with sophisticated aerodynamic criteria, so that flutter instability happens at appropriately high wind speed. In order to obtain decks with adequate behavior under wind loads, refined metallic carpentries (e.g. boxes with curved shapes) have to be adopted. In fact, although streamlined decks are known to be an effective solution against classical flutter instabilities, sophisticated numerical and experimental techniques to obtain an adequate aerodynamic optimization are often necessary, increasing the unit cost of the deck elements. The aim of the research proposed in this paper is to present some preliminary bridge designs, for which it is possible to obtain a total inhibition of the classical flutter instability mechanism in the wind speed range of interest. The basic idea is to avoid classical flutter by inverting the vertical bending and the torsional natural frequencies of the lower modes with similar shapes, that is to obtain torsional-to-vertical bending frequency ratios lower than one. This can be done by modifying the mass distribution over the deck with respect to the position of the suspension cables. Feasibility studies are shown, including analytical formulations, numerical strategies based on iterative non-linear Time History analysis and verifications by means of wind-tunnel tests. The results show that the proposed suspension bridge designs are not prone to classical flutter instability up to high wind velocities (80-100 m/s).*

## 1 INTRODUCTION

The present work deals with fluid-structure interaction of long-span bridges with multiple-box deck. These flexible structures are very sensitive to wind-induced loads, within both serviceability and ultimate limit states. In particular, it is extremely important to guarantee a reliable safety margin with respect to the collapse due to flutter. This aim can be pursued by improving the system stability from the aerodynamic point of view: multiple-box girder decks are known to be an effective solution in this direction (see e.g. Ref. [1]). Another common way to delay flutter instability is to increase the frequency separation (see e.g. Ref. [2,3]), thus working on the structural dynamics side of the problem.

An innovative solution would be the total inhibition of the flutter instability mechanism, at least concerning the lower modes, that is in the wind speed range of interest. This achievement could be very useful for future very-long-span bridges, for which any traditional countermeasure against flutter could have limited effects. The basic idea is to avoid classical flutter by inverting the vertical bending and the torsional natural frequencies of the lower modes with similar shapes (that is to obtain torsional-to-vertical bending frequency ratios lower than one), by a modification of the mass distribution over the deck with respect to the position of the suspension cables. As a matter of fact, if this was possible and compatible with all the design constraints, the effect of fluid-structure interaction would be the reduction with the wind speed of the torsional frequency and, at the same time, the increase of the vertical bending frequency: the modes would tend to further separate instead of coupling and consequently they could not give rise to classical flutter. This result is theoretically well known (see e.g. Ref. [2]) but completely unexplored in practice.

A feasibility study to understand the possibility to conceive reasonable structures with these characteristics has been the first step in this direction (Ref. [3]). In particular, the examined bridge solutions are based on the 1992-design of Messina Strait Bridge (see e.g. Refs. [4,5,6]). Keeping the main design philosophy, different configurations have been studied by varying the deck section and the cable suspension system.

The extensive study on the modal behavior of long-span suspension bridges, reported in Ref. [3], shows that the torsion-to-vertical bending frequency ratio is influenced not only by the mass distribution but also by the stiffness of the deck (usually considered as negligible with respect to the cable stiffness). In order to identify the scheme in which the frequency ratio is lower than unity, modal analyses have been performed on the bridge configurations examined in Section 3. The solution showing a twin-box girder deck with main cables closer one to each other and masses mainly placed on the outer sides of the suspension system, allows the suppression of flutter instability. It is also worth noting that twin-box girder sections have been recently selected or taken into account for several large bridge designs (e.g. Refs. [7,8]), due to their aerodynamic efficiency.

Wind-tunnel tests and numerical Time-History analysis have been performed too. Both experimental and numerical analysis (Sections 4 and 5) have confirmed the attainment of the aim against flutter instability.

In view of the results summarized herein, twin-box girder section is retained as an effective solution to design long-span suspension bridges with frequency ratios lower than one. In order to widen this study, further analyses are underway on both serviceability and ultimate limit states. In Section 6, first results concerning the maximum vertical and rotational deflections of the examined decks are shown.

## 2 FEASIBILITY STUDY

Two different suspension bridge typologies have been studied starting from the '92 design of Messina Strait Bridge, in order to obtain realistic proposals of suspension bridges, in terms of design criteria. The main span (3300 m), the side spans (960 m and 810 m), the maximum sag of the suspension cables (300 m) and the tower height (around 380 m) have not been changed, while the deck geometry, the distance between the main cables and the shape of the towers have been varied in order to obtain the following two configurations (Ref. [3]):

- (a) bridge with three suspension cables (Fig. 1);
- (b) bridge with two suspension cables closer to each other and masses mainly placed on the outer sides (Figs. 2 and 3).

The original grids between the boxes have not been considered within this study. Moreover, the total number of lanes have been reduced from three to two for each roadway.

In the case of configuration (a), the shape, the dimension, and the position of the road and railway boxes are the same as in the original design of 1992 (apart from the small widening of the railway box due to the introduction of a third hanger), whereas the cross beam can be conceived with reduced thicknesses (Fig. 1). The overall mass of the cables has been kept unchanged.

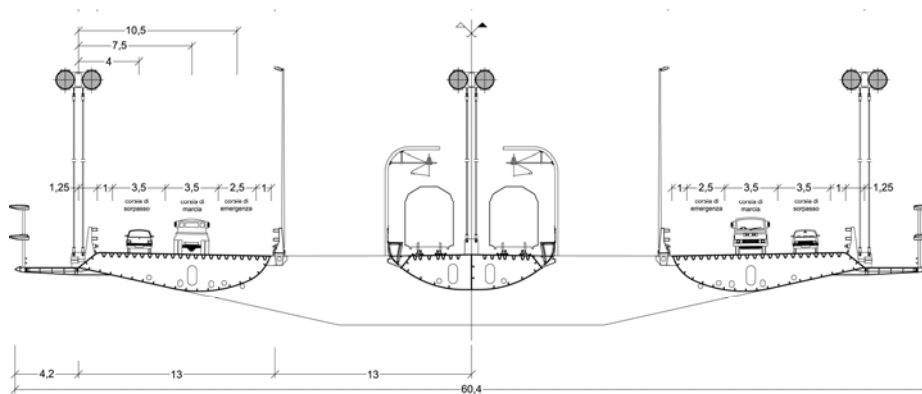


Figure 1: Three-box girder deck with three suspension cables

In the case of configuration (b), two different types of deck have been studied, that is with or without railways (Figs. 3 and 2 respectively). In the case of Fig. 2, the geometry of the road boxes is the same as the original one. However, in both cases the bending moments acting on the cross beam are lower than for configuration (a), so that the latter can be designed significantly smaller. The situation is even better in presence of the railways (Fig. 3).

The case studies shown in Fig. 2 have been obtained by changing the positions of cables and boxes. In particular:

- (b.1) the deck configuration (the one with 26 m gap between suspension cables) has been obtained from original Messina deck moving the suspension cables inside the road boxes;
- (b.3) the deck configuration (the one with 52 m gap between suspension cables) has been obtained from original Messina deck moving the suspension cables outside the road boxes;
- (b.2) the deck configuration (the one with 39 m gap between suspension cables) is an intermediate case.

Case studies showed in Fig. 3 have been obtained from the configurations (b.1), (b.2), and (b.3), after adapting the road boxes in order to accommodate railways.

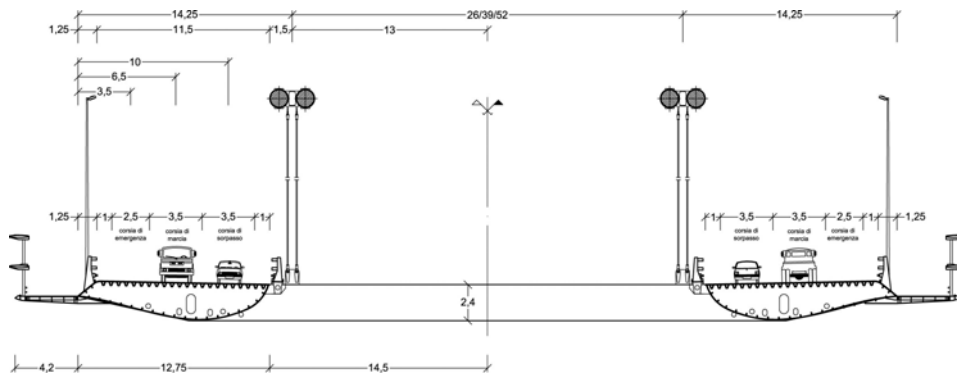


Figure 2: Twin-box girder deck with two suspension cables (spaced 26/39/52 m apart), without railway

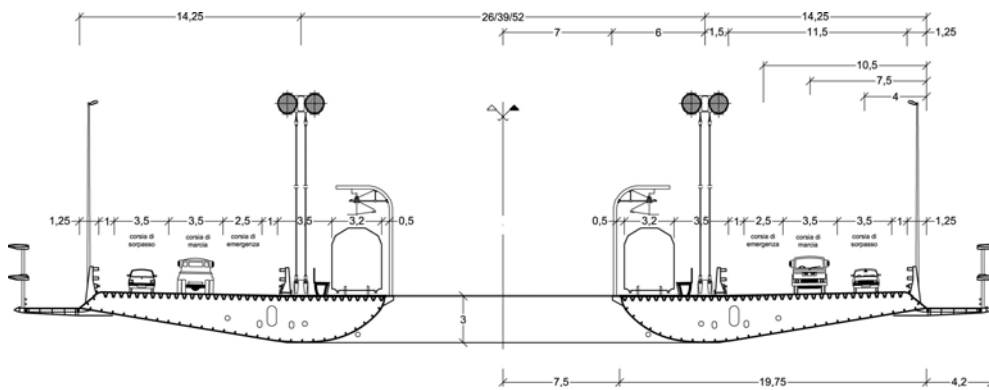


Figure 3: Twin-box girder deck with two suspension cables (spaced 26/39/52 m apart), with railway

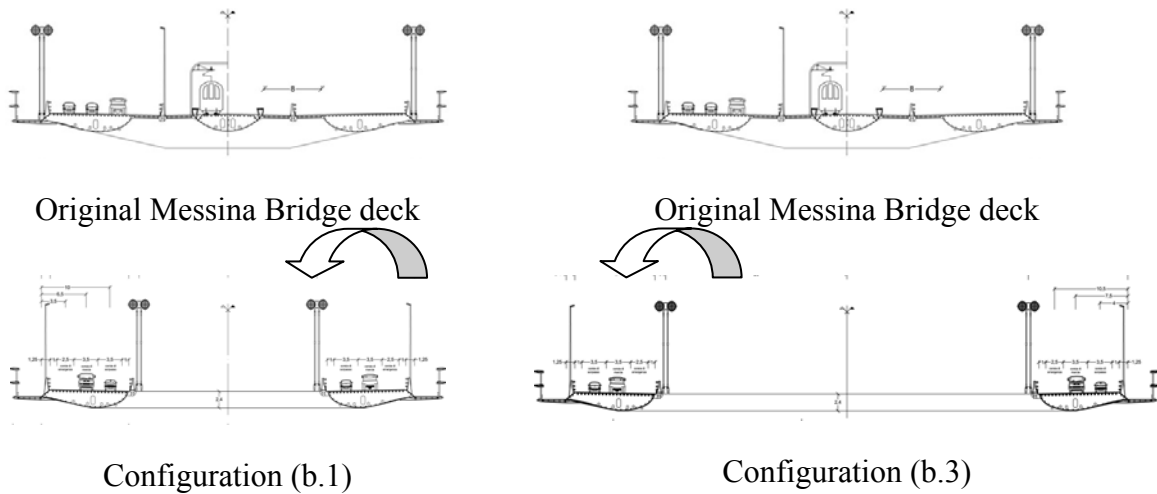


Figure 4: Comparison between original Messina bridge's deck and the proposed two twin-box girder's decks with two suspension cables spaced 26 and 52 m, without railway

### 3 MODAL ANALYSIS RESULTS

In order to evaluate the frequency ratio between vertical and torsional modes of configurations (a) and (b), different finite element numerical models of global structures have been set

up. Each model is made of 1006 joints, 588 cable elements and 924 frame elements (Fig. 5). The geometrical and mechanical characteristics of the towers and of transversal boxes of the decks have been evaluated taking into account the actual new permanent loads and mass distributions. The geometrical and mechanical characteristics of longitudinal boxes are the same as the original Messina Bridge.

Numerical results for configuration (a) show that the presence of the central cable does not allow to invert the natural frequencies. As a matter of fact, it is possible to obtain a frequency ratio equal to 1.10 only by assigning almost the total mass (90 %) to the central cable, which is obviously just a mathematical abstraction (Ref. [1]).

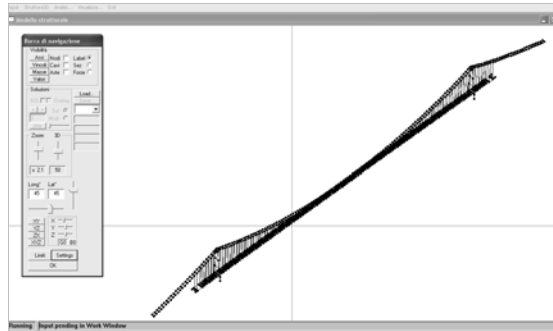


Figure 5: Numerical global models of configuration denoted as (b.1), (b.2) and (b.3)

Conversely, it is possible to invert the modal frequencies by adopting the configurations (b.1), (b.2) and (b.3). This holds true also if the distance between the cables is increased from 26 m to 39 m and then to 52 m: in these last cases, the bending moment on the cross beam slightly increases, whereas the deck rotation is reduced.

In view of the results summarized herein, configurations denoted as (b.1), (b.2) and (b.3) are retained as effective solutions to design long-span suspension bridges with frequency ratios lower than one (Fig. 6 and Tab. 1). Even if the 1<sup>st</sup> torsional-to-1<sup>st</sup> bending frequency ratio is about one in still air, the attainment of the aim against flutter instability is substantially obtained. In fact, it is known that the frequency separation is expected to increase under wind as a consequence of the reduction of the torsional frequency and, at the same time, of the slight increase of the vertical bending frequency. Consequently, the modes should tend to further separate instead of coupling, thus not giving rise to classical flutter. Moreover, the achievement of the aim flutter-instability suppression is confirmed by the 2<sup>nd</sup> torsional-to-2<sup>nd</sup> bending frequency ratio, that is smaller than one for all the examined configurations.

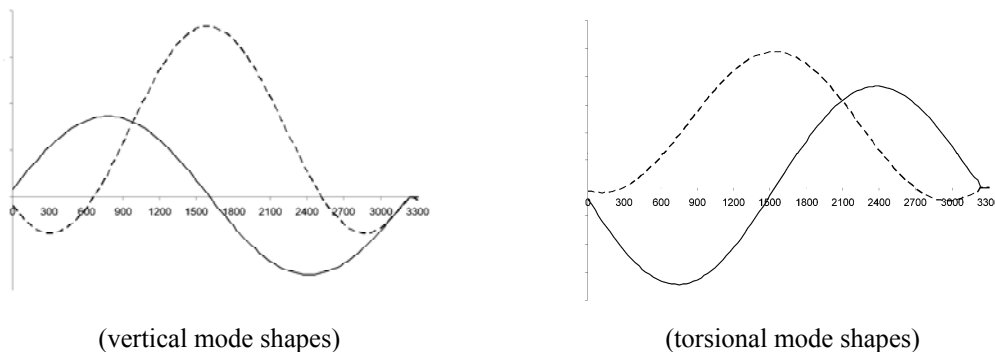


Figure 6: Modal shapes for configurations denoted as (b.1), (b.2) and (b.3)

Modal analysis on twin-boxes decks of bridges with railways are underway. First numerical results on section models show that it is possible to obtain torsional-to-bending frequency ratios smaller than one if the centres of gravity of the boxes are external with respect to the suspension cable planes.

Configuration (b.1)		Configuration (b.2)		Configuration (b.3)	
Mode shape	$f$ [Hz]	Mode shape	$f$ [Hz]	Mode shape	$f$ [Hz]
1 <sup>st</sup> torsional	0.06052	1 <sup>st</sup> torsional	0.06077	1 <sup>st</sup> torsional	0.06192
1 <sup>st</sup> vertical	0.06074	1 <sup>st</sup> vertical	0.06099	1 <sup>st</sup> vertical	0.06181
2 <sup>nd</sup> torsional	0.07731	2 <sup>nd</sup> torsional	0.07720	2 <sup>nd</sup> torsional	0.07814
2 <sup>nd</sup> vertical	0.08211	2 <sup>nd</sup> vertical	0.08201	2 <sup>nd</sup> vertical	0.08197

Table 1: Modal frequencies for configurations denoted as (b.1), (b.2) and (b.3)

#### 4 EXPERIMENTAL CAMPAIGN

In order to characterize the aerodynamic properties of the conceived bridge deck section and verify the actual stability of a system with frequency ratio lower than one, excluding the onset of unknown phenomena, a series of wind-tunnel tests has been performed in the CRIACIV Boundary Layer Wind Tunnel in Prato, Italy. This facility has a test section 2.42 m large and 1.60 m high. Wind speeds up to 30 m/s are possible. The wooden section model shown in Fig. 7 has been used for the tests: it is 2.33 m long and 0.562 m large, so that the geometric scale with respect to the deck (b.1) described in Section 2 is about 1:92.5.



Figure 7: Section model tested in the CRIACIV wind tunnel

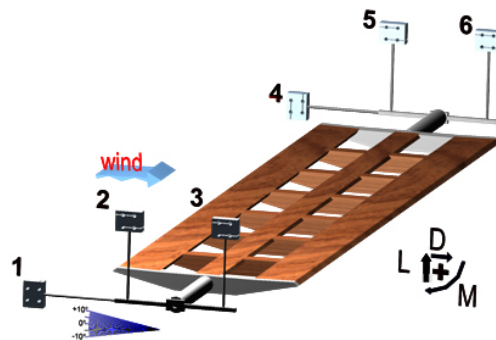


Figure 8: Scheme of the set-up used for the static tests

Aerodynamic force coefficients have been measured by means of the static set-up shown in Fig. 8, consisting of six load transducers (strain-gauges ones) supporting the section model through a system of connecting rods.

Results for various angles of attack are shown in Fig. 9 for the bare deck and for the configuration with lateral spoilers [see Fig. 7]. The presence of the spoilers increases the very low drag of this section profile and slightly modifies the moment coefficient, whereas it has practically no effects on the lift coefficient. Fig. 10 shows that the aerodynamic forces relative to this twin-box girder deck are close to those measured for the corresponding three-box girder (Ref. [1]); as expected, the major differences are affecting the moment coefficient.

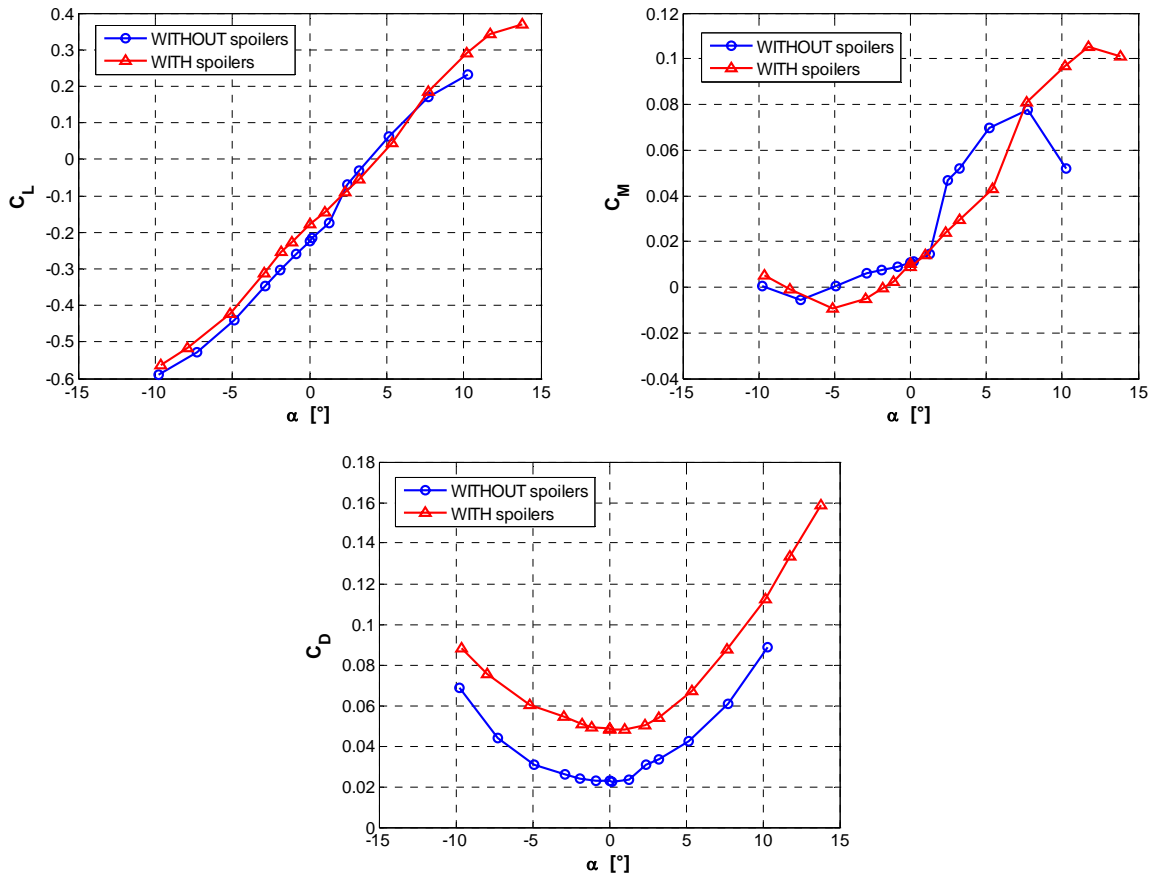


Figure 9: Aerodynamic force coefficients for the deck configurations with ( $Re_B = 700,000$ ) and without spoilers ( $Re_B = 800,000$ )

The effect of Reynolds number variation has been also investigated and, similarly to the three-box girder deck, it is found that in the wind-tunnel range this is very pronounced for the bare deck case, while it is milder in the configuration with spoilers, as clearly shown in Fig. 11. In addition, no significant Reynolds number effects have been encountered between  $Re_B = 700,000$  and  $900,000$ . Particularly interesting are the lift and moment slopes around  $\alpha = 0^\circ$ , positive in both cases, that are used in the next Section to define the quasi-steady self-excited load to be used in the numerical computation of the bridge deck stability.

Aeroelastic tests have been also performed by using the two-degree-of-freedom set-up described in details in Ref. [9]. The section model is clamped to rigid support arms and then elastically suspended by means of a system of eight springs and steel cables. The along wind degree of freedom is restrained with long anti-drag cables connected to the model by means of low-friction roll bearings. The model is let free to oscillate for the effect of low wind-tunnel

turbulence and signature turbulence and vertical displacements and rotations are monitored with three laser displacement transducers. A scheme and a picture of the set-up are reported in Figs. 12-13. The pitching-to-heaving frequency ratio of the mechanical system is controlled by varying the distance between the springs in the along-wind direction.

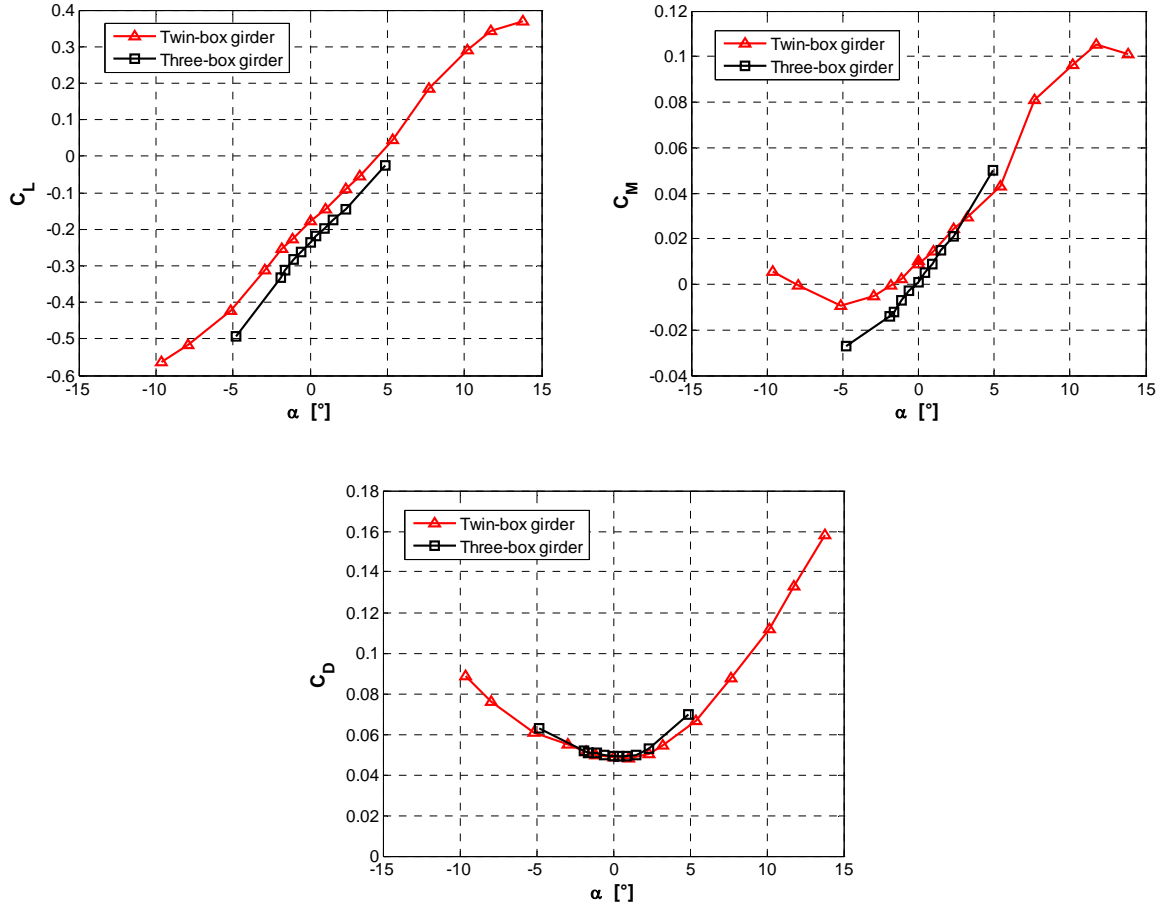


Figure 10: Comparison between the aerodynamic force coefficients measured for the twin-box ( $Re_B = 700,000$ ) and the three-box girder ( $Re_B = 620,000$ ) section models in the configuration with spoilers

Four model configurations have been tested, differing for the pitching-to-heaving frequency ratio  $\gamma_\omega = f_\alpha/f_h$ , ranging from 0.789 to 1.000, the presence or not of the lateral spoilers and the initial still-air angle of attack  $\alpha_0$ . The list of configurations and corresponding results are reported in Tab. 2 and Fig. 14. It can be remarked that for both Conf-1 and Conf-3 only static torsional divergence appears at very high reduced wind speed. In the case of Conf-4 (bare-deck section model) the test has been interrupted before the onset of any instability, due to the very large deformation of the springs. Only in the case of Conf-2, where a large initial positive angle of attack is imposed, a dynamic instability appeared. This is single-degree of freedom torsional flutter, due to the very large angle of incidence (around  $12^\circ$ ) and the consequent fully stalled behavior of the deck profile. It is also worth noting that in the case of Conf-3, due to the significant mean angle of attack, large heaving oscillation amplitudes are observed for reduced wind speeds  $U/Bf_{\alpha 0}$  beyond about 14. Fig. 15 shows that the pitching-mode frequency decreases with increasing wind speed, while the heaving one remains substantially unchanged. This means that, as expected, the frequency separation is enhanced by the self-



excited load and the modes do not tend to couple. Finally, the aeroelastic tests confirm the theoretical result according to which coupled flutter instability cannot arise in systems with frequency ratio lower or equal to unity. In addition, no unexpected phenomena have been observed.

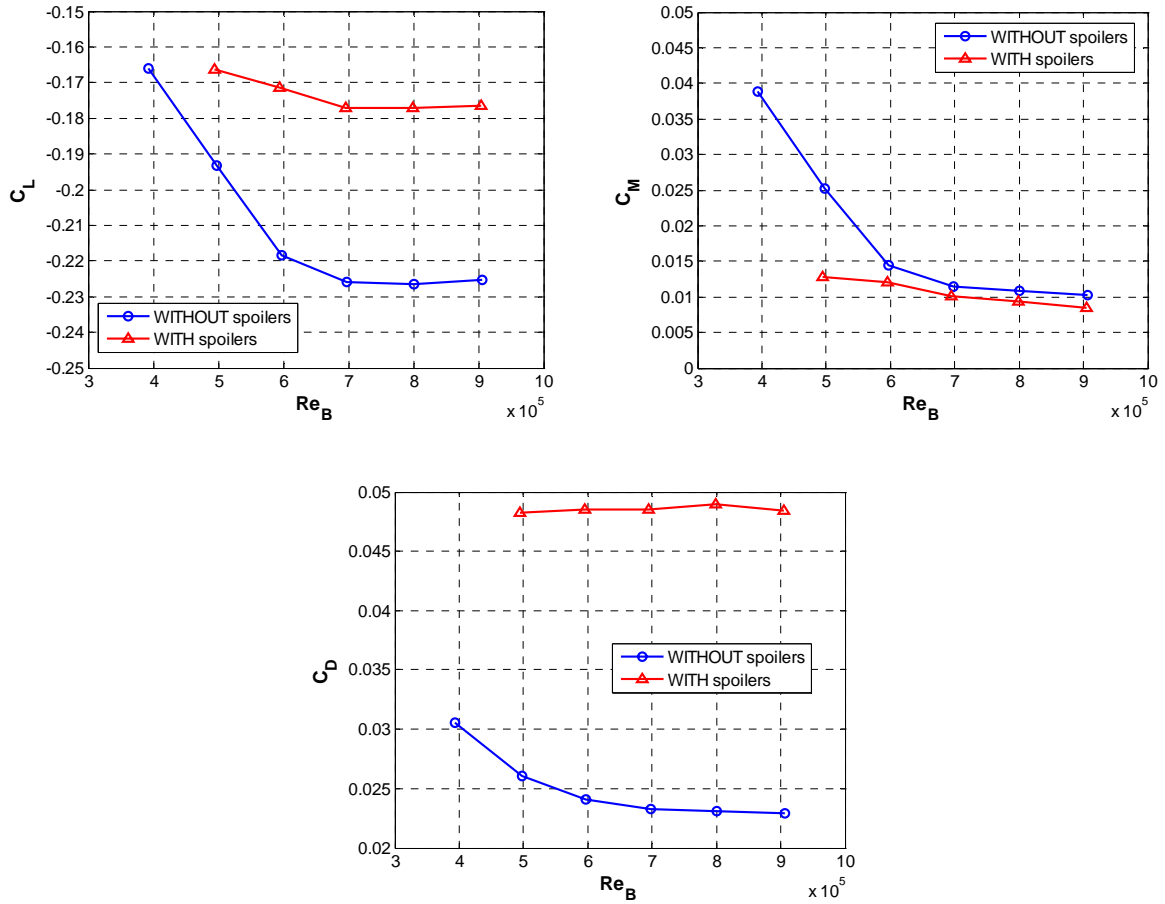


Figure 11: Dependence on Reynolds number of the aerodynamic force coefficients ( $\alpha = 0^\circ$ )

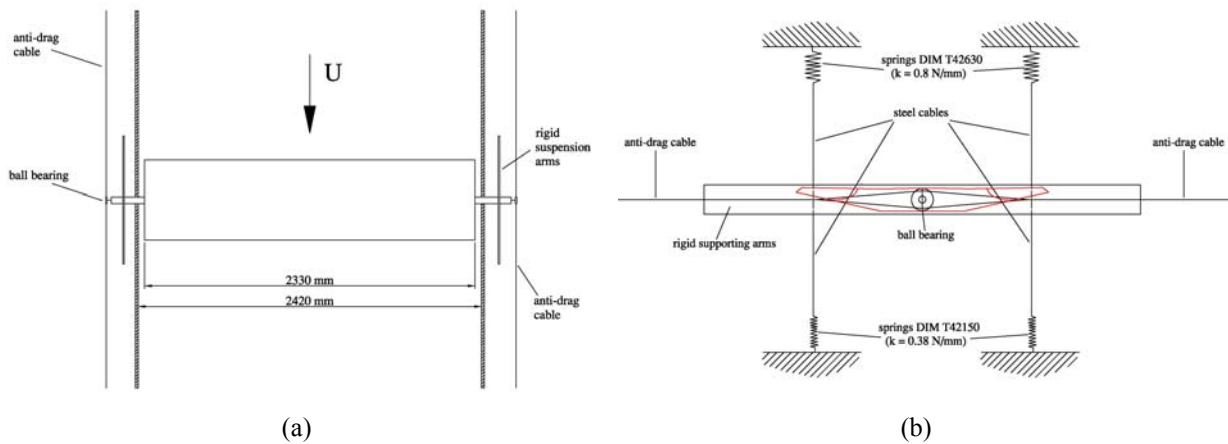
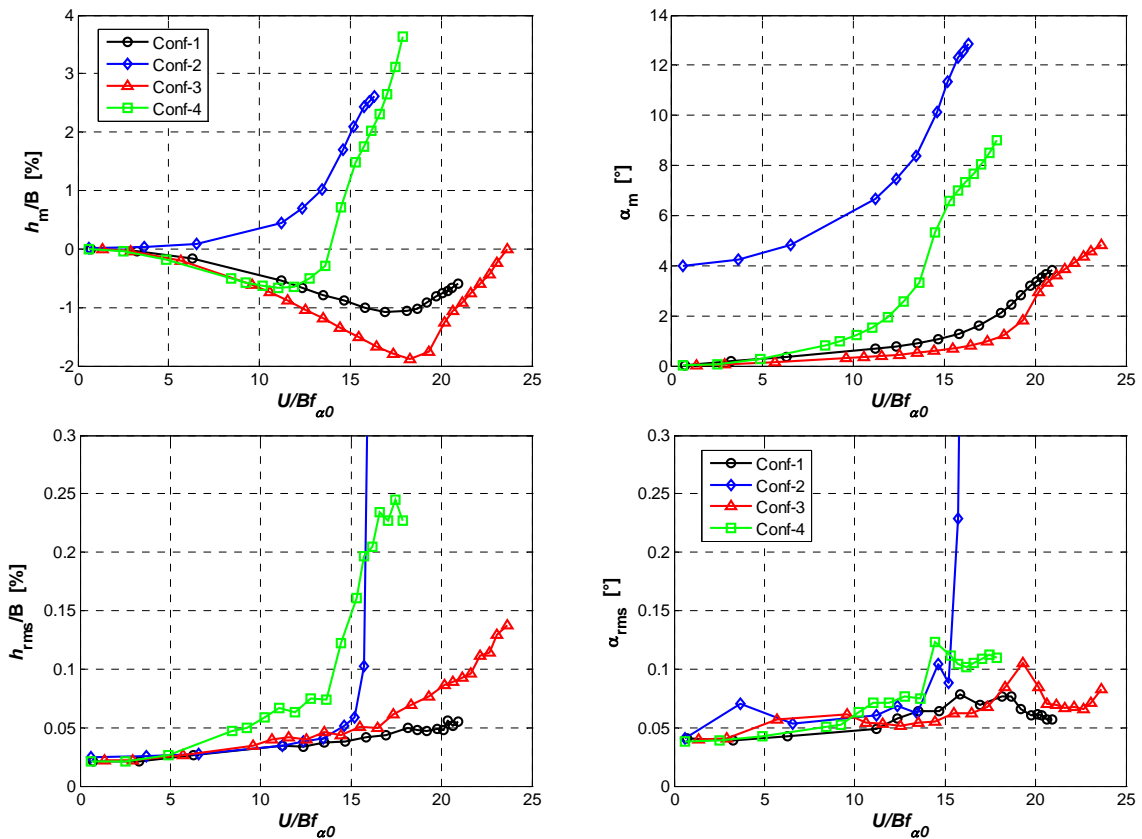


Figure 12: (a) Top and (b) lateral schematic views of the aeroelastic set-up



Figure 13: Lateral view of the elastic suspension system for the aeroelastic tests


 Figure 14: Mean and RMS values of vertical displacement ( $h$ ) and rotation ( $\alpha$ ) of the elastically suspended section model at various wind speeds.  $f_{\alpha 0}$  is the still-air pitching frequency

	Spoilers	$\alpha_0$ [°]	$\gamma_\omega$	$f_{h0}$ [Hz]	$f_{\alpha 0}$ [Hz]	$U_c$ [m/s]	$U_{Rc}$ [-]	Instability
<b>Conf-1</b>	yes	0	0.789	2.18	1.71	20.3	21.1	TD
<b>Conf-2</b>	yes	+4.3	0.789	2.18	1.71	15.4	16.0	TF
<b>Conf-3</b>	yes	0	0.920	2.18	2.02	27.4	24.1	TD
<b>Conf-4</b>	no	0	1.000	2.27	2.27	> 22.8	> 17.9	NR

 Table 2: Configurations tested with the aeroelastic set-up.  $U_c$  and  $U_{Rc}$  are respectively the critical and the reduced critical wind speeds.  $\alpha_0$  is the initial (still air) angle of attack,  $f_{h0}$  e  $f_{\alpha 0}$  are respectively the still-air heaving and pitching frequencies. TD = torsional divergence; TF = torsional flutter; NR = not reached

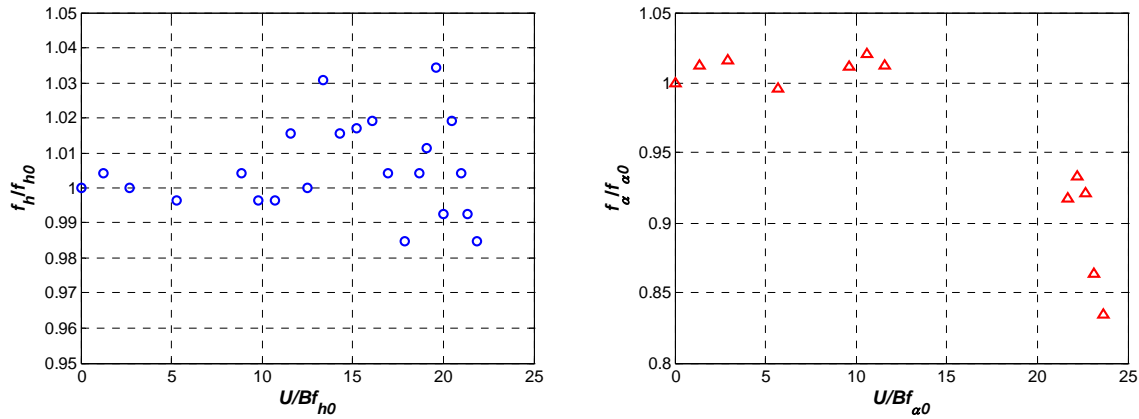


Figure 15: Heaving and pitching frequency evolution with the wind speed for test case Conf-3

## 5 TIME-HISTORY ANALISYS RESULTS

In support of modal and experimental studies, Time-History analyses have been performed on the global numerical models referring to configurations (b.1) and (b.3) described in Section 3. The self-excited forces acting on the deck are obtained from the static aerodynamic coefficients shown in Section 4 (Fig. 9) following the Quasi-Steady analytical method (see e.g. Ref. [3]). For each numerical model, the duration of the dynamical analysis is 1000 seconds and the duration of the linear ramp of the wind speed is 10 seconds (this is a very severe way to test the numerical stability).

The analysis results show that flutter instability does not occur up to high wind speeds for both configurations (b.1) and (b.3). In Figs. 17 and 18, Time-History analysis results are shown for the configuration (b.3) under a wind speed of 90 m/s, being  $F_y$  and  $F_z$  respectively the drag and lift aeroelastic forces on the bridge deck,  $M_x$  the aeroelastic moment with respect to the longitudinal x-axis of the deck,  $S_z$  the vertical displacement of the deck,  $V_y$  the horizontal velocity and  $R_x$  the rotation around the longitudinal axis, all referring to the sign convention of Fig. 16.

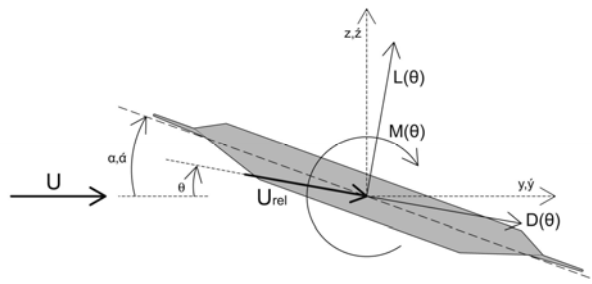


Figure 16: Sign convention for forces, displacements and velocities

In particular, the aeroelastic forces in Fig. 17 refer to the experimental model without spoilers, whereas the aeroelastic forces in Fig. 18 are obtained from the static coefficients measured for the model with spoilers. Although large static deflections are evident over 100 m/s wind velocity for both bridge configurations, no flutter instability occurs in the wind speed range of interest.

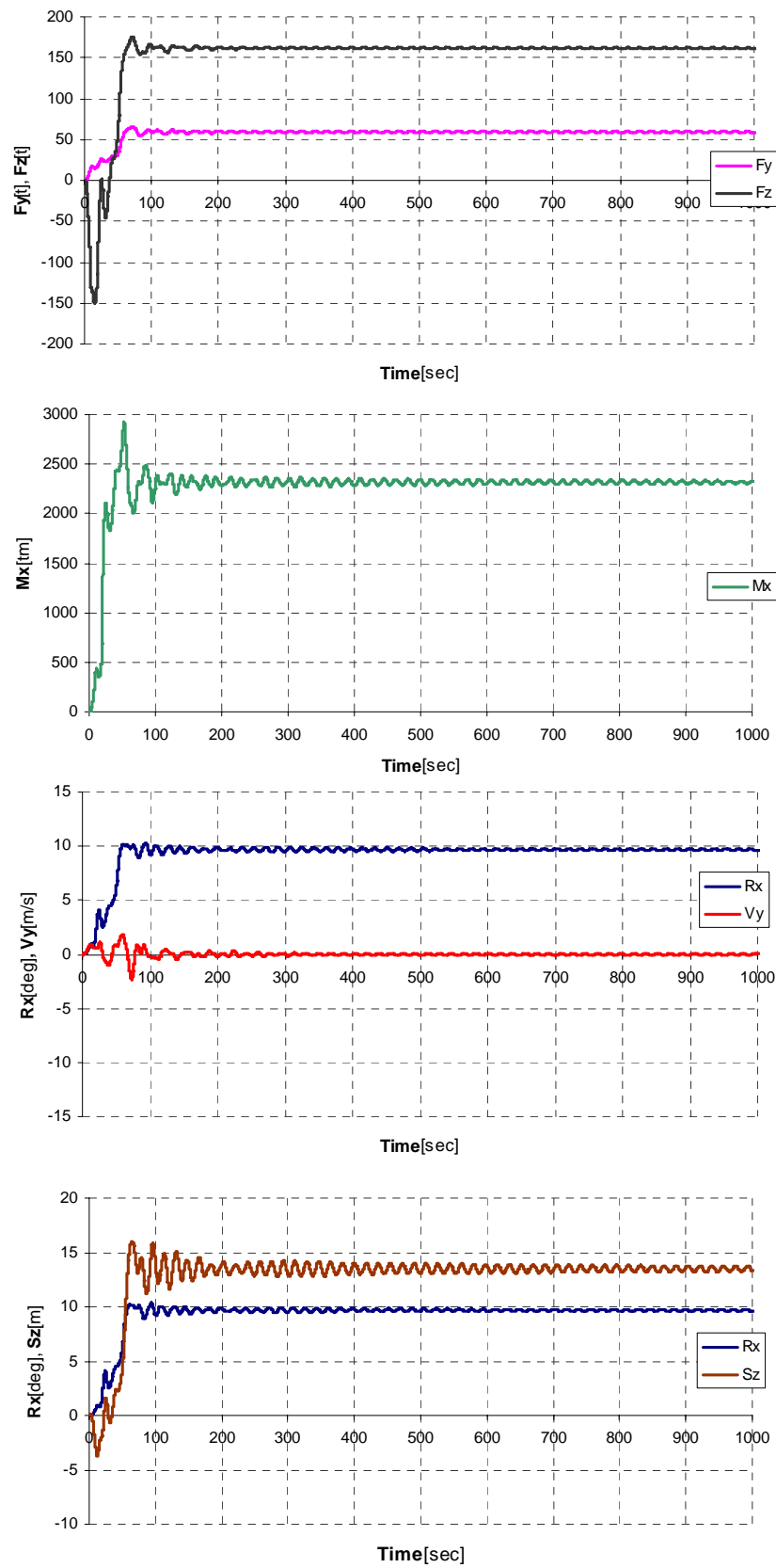


Figure 17: Time History results for configuration denoted as (b.3) without spoilers at 90 m/s wind velocity

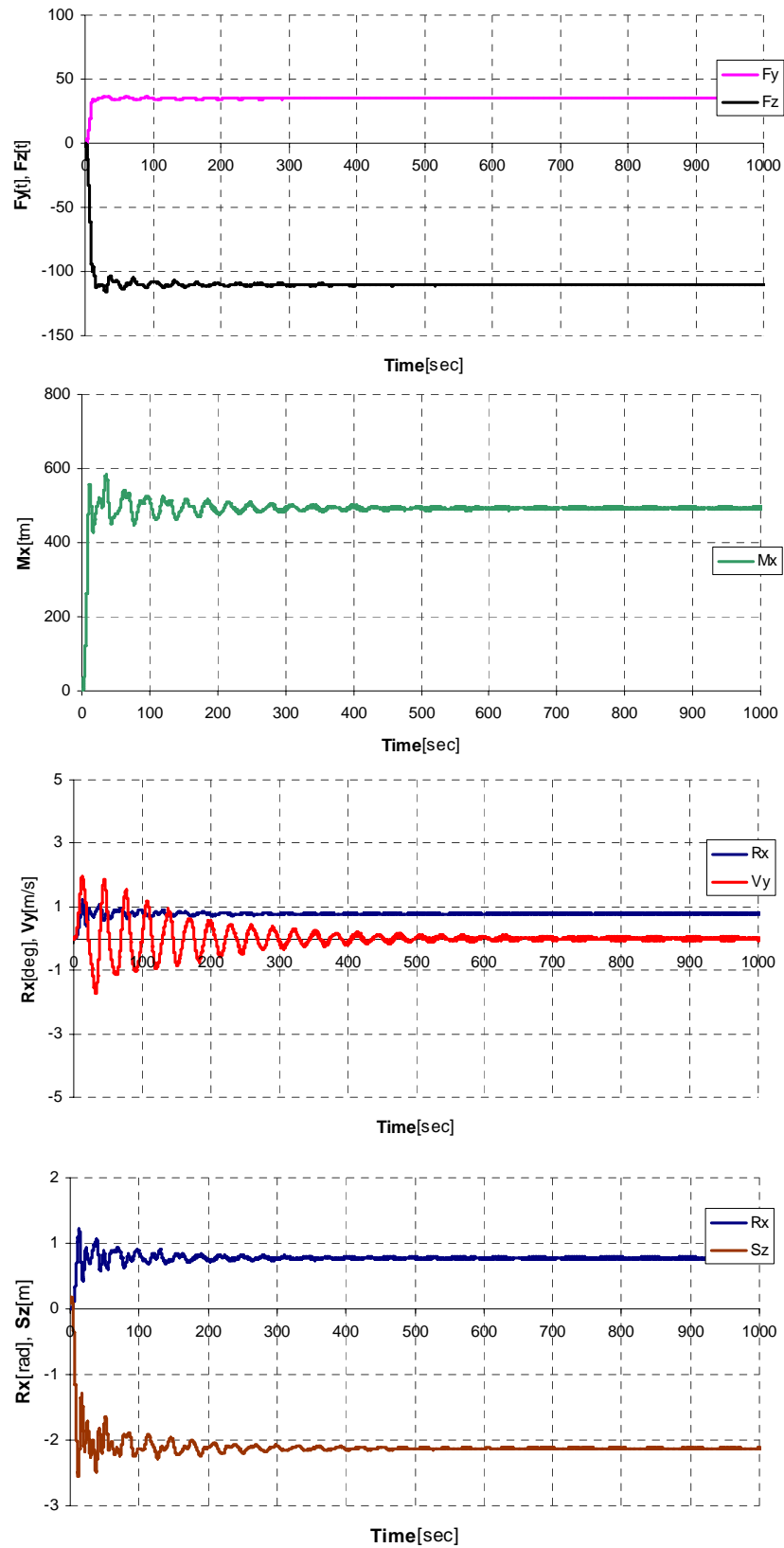


Figure 18: Time History results for configuration denoted as (b.3) with spoilers at 90 m/s wind velocity

## 6 SERVICEABILITY STUDY RESULTS

In order to widen this study, further analyses have been made on serviceability limit state, concerning, for instance, the maximum static vertical and rotational deflections of the deck. In particular, the load conditions tested on numerical global models described in Section 3 are the ones represented in Figs. 19-20.

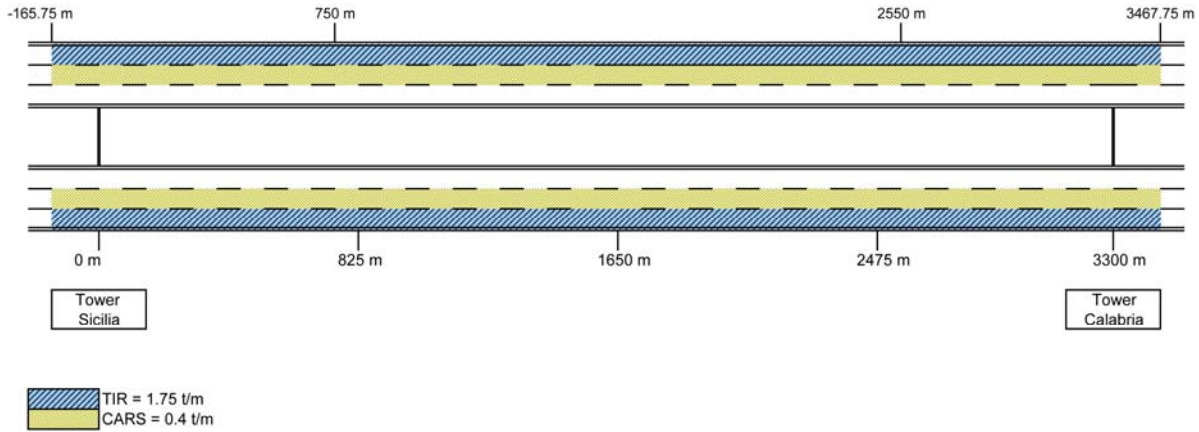


Figure 19: Load condition 1 (LC1) for static analysis of configurations denoted as (b.1), (b.2) and (b.3)

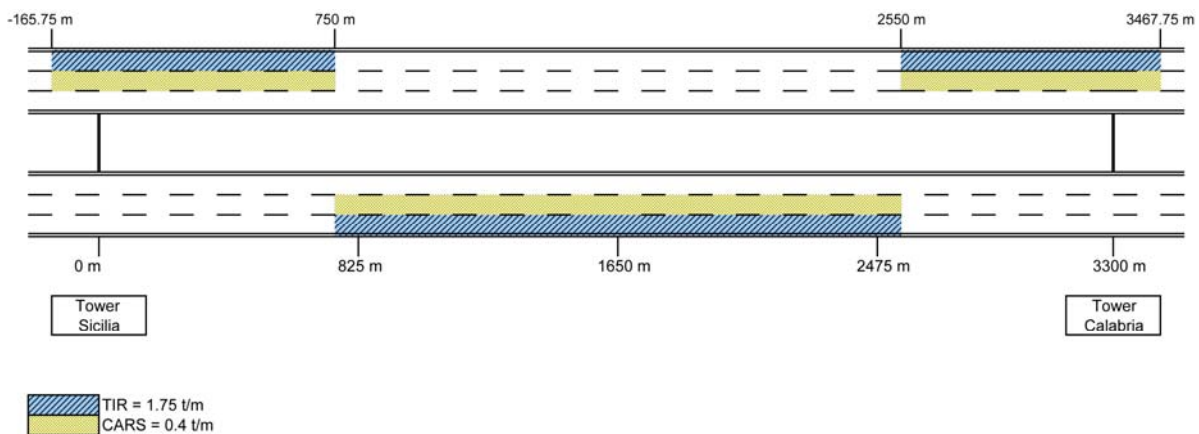


Figure 20: Load condition 2 (LC2) for static analysis of configurations denoted as (b.1), (b.2) and (b.3)

The results of static analysis for configurations (b.1), (b.2) and (b.3) under LC1 load condition show that both vertical and torsional deck deflections are acceptable (all values of deck slope are below 1%) and fall within the specifications used for the original '92 Messina Bridge design.

On the other hand, the results of static analysis for the configurations (b.1), (b.2) and (b.3) under the particularly burdensome LC2 load condition show that, while vertical deck deflections are acceptable (all values of deck slope are below 1%), torsional deflections do not respect the limitation required by Messina Bridge design specifications. Nevertheless, since the transversal deck slope tends to the extreme value of 8% in the case of configurations (b.3) (Fig.21), the possibility to increase the distance between the suspension cables seems to be a not too expensive solution to reduce the deck deflections according to the original specifications.

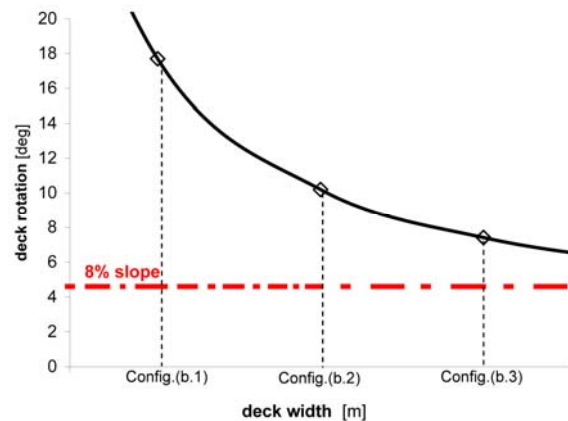


Figure 21: Torsional deck deflections of configurations (b.1), (b.2) and (b.3) under LC2 load condition

## 7 CONCLUSIONS

In this paper the possibility of avoiding flutter instability by inverting the vertical bending and the torsional eigenfrequencies is investigated. Preliminary numerical studies show that such a bridge can be reasonably designed and the selected solution is a twin-box girder deck with masses mainly placed externally with respect to the suspension system. It is worth noting that this typology of multiple-box deck sections can be also very performing from the aerodynamic point of view, if correctly designed. The aeroelastic behavior of structures with frequency ratios lower than one has been both numerically and experimentally studied. No unexpected aeroelastic phenomena have been observed, while single-degree-of-freedom torsional flutter has been observed in the wind-tunnel only under extreme conditions, not significant from a design point of view.

## ACKNOWLEDGEMENTS

The research work has been partially performed in the framework of the Italian National Research Contract (PRIN) “AER-BRIDGE: Aeroelastic Phenomena and Other Dynamic Interactions on Non-Conventional Bridges and Footbridges”, two-year grant from the Italian Ministry of University and Scientific Research (MIUR).

## REFERENCES

- [1] G. Bartoli, P. D'Asdia, S. Febo, C. Mannini, S. Pastò and L. Procino. Innovative solutions for the design of long-span bridges: investigations on the aeroelastic behavior of multiple-box girder deck sections. Proceedings of the XII International Conference on Wind Engineering, pp. 2359–2366, Cairns, Australia, July 1-6, 2007.
- [2] C. Dyrbye and S. Hansen. *Wind loads on Structures*. John Wiley & Sons, New York, 1997.
- [3] S. Febo. Impalcati e schemi strutturali per ponti di grandissima luce. Ph.D. Thesis, University of Pescara, Italy, 2007 (in Italian).

- [4] F. Brancaleoni and G. Diana. The aerodynamic design of the Messina Strait Bridge. *Journal of Wind Engineering and Industrial Aerodynamics*, **48**(2-3), 395–409, 1993.
- [5] G. Diana, M. Falco, S. Bruni, A. Cigada, G.L. Larose, A. Damsgaard and A. Collina. Comparisons between wind tunnel tests on a full aeroelastic model of the proposed bridge over Stretto di Messina and numerical results. *Journal of Wind Engineering and Industrial Aerodynamics*, **54–55**, 101–113, 1995.
- [6] P. D'Asdia and V. Sepe. Aeroelastic instability of long span suspended bridges: a multi-mode approach. *Journal of Wind Engineering and Industrial Aerodynamics*, **74–76**, 849–857, 1998.
- [7] G.L. Larose, S.V. Larsen, A. Larsen, M. Hui and A.G. Jensen. Sectional model experiments at high Reynolds number for the deck of a 1018 m span cable-stayed bridge. Proceedings of the XI International Conference on Wind Engineering, pp. 373–380, Lubbock, USA, June 2-5, 2003.
- [8] K. Ogawa, H. Shimodoi and T. Oryu. Aerodynamic characteristics of a 2-box girder section adaptable for a super-long span suspension bridge. *Journal of Wind Engineering and Industrial Aerodynamics*, **90**, 2033–2043, 2002.
- [9] C. Mannini. *Flutter vulnerability assessment of flexible bridges*. Ph.D. Thesis, University of Florence, Italy - TU Braunschweig, Germany, 2006
- [10] R.H. Scanlan and J.J. Tomko. Airfoil and bridge deck flutter derivatives. *Journal of Engineering Mechanics Div. Proc. ASCE*, **97**(EM6), 1717–1737, 1971
- [11] P.P. Sarkar, N.P. Jones and R.H. Scanlan. System identification for estimation of flutter derivatives, *Journal of Wind Engineering and Industrial Aerodynamics*, **41–44**, 1243–1254, 1992